THERAPEUTIC HYPOTHERMIA AND TEMPERATURE MANAGEMENT
Volume 3, Number 2, 2013

DOI: 10.1089/ther.2013.0001

DNA Microarray Analysis of the Mouse Adrenal Gland for the Detection of Hypothermia Biomarkers: Potential Usefulness for Forensic Investigation

Masataka Takamiya,[1] Kiyoshi Saigusa,[2] and Koji Dewa[1]

We analyzed the adrenal gland transcriptome of mice killed by hypothermia using DNA microarray technology. A total of 4051 significantly expressed genes were identified; 2015 genes were upregulated and 2036 were downregulated. The FBJ osteosarcoma oncogene was the most upregulated, whereas stearoyl coenzyme A desaturase 3 was the most downregulated. Validation by quantitative polymerase chain reaction revealed that results obtained by both methods were consistent. In the gene set analysis, significant variations were found in nine pathways, and we suggest that transforming growth factor β and tumor necrosis factor α would be involved in the pathogenesis of hypothermia. Gene functional category analysis demonstrated the most overexpressed categories in upregulated and downregulated genes were cellular process in biological process, binding in molecular function, and cell and cell part in cellular component. The present study demonstrated acute adrenal responses in hypothermia, and we suggest that understanding adrenal mRNA expression would be useful for hypothermia diagnosis. Furthermore, the present microarray data may also facilitate development of immunohistochemical analysis of human cases. In forensic practice, the combination of macroscopic and microscopic observations with molecular biological analyses would be conducive to more accurate diagnosis of hypothermia. Although this study is aimed at forensic practice, the present data regarding more than 20,000 genes of the adrenal gland would be beneficial to inform future clinical hypothermia research. From the viewpoint of adrenal gene activity, they could contribute to elucidating the pathophysiology of hypothermia.

Introduction

Hypothermia is classically defined as a core body temperature of less than 35°C. Hypothermia develops when the adaptive mechanism is overwhelmed (Ulrich and Rathlev, 2004), and it is generally understood that hypothermia is a common and widespread danger even in temperate climates, outside and indoors (Saukko and Knight, 2004). Numerous hypothermia cases are reported every year in areas that are typically considered to have warm weather, such as Florida, Texas, California, and Alabama (Ulrich and Rathlev, 2004).

Forensic pathologic diagnosis of hypothermia involves some difficult issues. Diuresis (Paton, 1983) and hypoglycemia (DiMaio and DiMaio, 2001) occur in the early phase of hypothermia. Peripheral vasoconstriction is the main cause of frostbite (Saukko and Knight, 2004). Hypothermia may cause all of the following: bright pink lividity; hemorrhagic pancreatitis; erosions and hemorrhages in the gastric mucosa, ileum, and colon; bronchopneumonia; acute tubular necrosis; cardiac muscle degeneration (DiMaio and DiMaio, 2001); pulmonary edema; deep vein thrombosis (Saukko and Knight, 2004); and hemorrhage in muscles (Aghayev *et al.*, 2008). These autopsy findings are not specific to hypothermia. Therefore, diagnosis must be based partly on exclusion and by relying on historical information, and it is thought that molecular biological analyses could provide more valuable information (Hirvonen and Huttunen, 1982). Some hormonal changes of the adrenal gland were reported in hypothermia (Hirvonen and Lapinlampi, 1989; Hirvonen and Huttunen, 1995), and we considered it worthwhile to analyze the transcriptome. In this study, the transcriptome of the adrenal gland in hypothermia was analyzed, to evaluate its utility for the diagnosis of hypothermia. Although this study is aimed at forensic practice, the present gene expression analysis would be beneficial for use in clinical hypothermia research.

Materials and Methods

Tissue samples

The water bath model (Okuda *et al.*, 1986) was adapted. Male ddY mice, 7 weeks of age, weighing 35.4 ± 5.6 g, were housed under controlled lighting (lights on at 7:00 am and off at 7:00 pm) and given free access to food and water. The mice were anesthetized by sevoflurane inhalation, and confined in a metallic restraint cage which was kept in a water bath at 10°C, so that the neck was immersed. The animals were sacrificed by continuous exposure to cold water (41.4 ± 10.6 minutes). The left adrenal gland was resected ($n = 4$ for DNA microarray, $n = 4$ for internal standard gene selection, $n = 10$

Departments of [1]Forensic Medicine and [2]Biology, Iwate Medical University, Iwate, Japan.

Table 1. Upregulated Genes of the Adrenal Gland Arranged by Decreasing Fold Change

Probe name	*Signal intensity in hypothermia*	*Fold change*	*Description*	*Symbol*	*RefSeq*
A_52_P262219	5521.219425	33.69810362	FBJ osteosarcoma oncogene	*Fos*	NM_010234
A_55_P2054261	1270.285775	11.82976984	C2 calcium-dependent domain containing 4B	*C2cd4b*	NM_001081314
A_51_P415395	1512.015738	9.380546663	C2 calcium-dependent domain containing 4B	*C2cd4b*	NM_001081314
A_51_P260683	474.996815	6.745736195	Regulator of G-protein signaling 1	*Rgs1*	NM_015811
A_51_P430900	4371.102825	6.465845343	Dual specificity phosphatase 1	*Dusp1*	NM_013642
A_55_P2011106	437.44096	6.416245306	Jun-B oncogene	*Junb*	NM_008416
A_51_P367866	18185.9535	5.489176391	Early growth response 1	*Egr1*	NM_007913
A_55_P2181341	423.2009575	4.483405844	Endothelin converting enzyme-like 1	*Ecel1*	NM_021306
A_51_P252859	1538.858175	4.395378178	Cysteine rich protein 61	*Cyr61*	NM_010516
A_51_P212782	391.7808825	4.119763443	Interleukin 1 beta	*Il1b*	NM_008361
A_52_P31543	4632.8834	4.071461048	B-cell translocation gene 2, anti-proliferative	*Btg2*	NM_007570
A_55_P2181191	189.892655	4.033899105	B-cell translocation gene 1, anti-proliferative	*Btg1*	NM_007569
A_55_P2408588	1335.50504	3.961004115	Aryl hydrocarbon receptor nuclear translocator-like	*Arntl*	NM_007489
A_51_P140710	405.8231625	3.803014132	Chemokine (C-C motif) ligand 3	*Ccl3*	NM_011337
A_55_P2031272	105.2809935	3.534519497	LIM homeobox protein 3	*Lhx3*	NM_001039653
A_55_P2351193	130.6831425	3.1072758	Small nucleolar RNA, H/ACA box 47	*Snora47*	NR_034043
A_51_P245796	29637.41075	2.834485718	DNA-damage-inducible transcript 4	*Ddit4*	NM_029083
A_66_P116173	178.1135225	2.80506208	Interleukin 23 receptor	*Il23r*	NM_144548
A_51_P264695	2077.4311	2.745770413	Crystallin, mu	*Crym*	NM_016669
A_55_P2147897	208.78882	2.684448635	C2 calcium-dependent domain containing 4A	*C2cd4a*	NM_001163143
A_51_P497395	289.0736275	2.653749694	Ly6/Plaur domain containing 1	*Lypd1*	NM_145100
A_51_P108659	1013.009025	2.651716606	Paraoxonase 1	*Pon1*	NM_011134
A_51_P286488	730.3182925	2.649214941	Immediate early response 3	*Ier3*	NM_133662
A_51_P363187	117.7416945	2.64447255	Chemokine (C-X-C motif) ligand 1	*Cxcl1*	NM_008176
A_52_P608495	872.8185	2.575860386	Alanyl-tRNA synthetase 2, mitochondrial (putative)	*Aars2*	NM_198608
A_55_P2112642	315.61053	2.501941401	Thyroid stimulating hormone receptor	*Tshr*	NM_001113404, NM_011648
A_51_P315904	13396.8485	2.458968067	Growth arrest and DNA-damage-inducible 45 gamma	*Gadd45g*	NM_011817
A_55_P2113051	360.0429375	2.458243622	FBJ osteosarcoma oncogene B	*Fosb*	NM_008036
A_52_P80944	209.3950225	2.453644777	Zinc finger protein 36	*Zfp36*	NM_011756
A_55_P2073248	563.57966	2.434264777	Solute carrier family 25, member 34	*Slc25a34*	NM_001013780
A_55_P2163028	443.7092425	2.432368649	Immediate early response 2	*Ier2*	NM_010499
A_55_P1985693	188.4100325	2.39929641	FH2 domain containing 1	*Fhdc1*	NM_001033301
A_52_P536494	888.75921	2.367826545	v-myc myelocytomatosis viral related oncogene, neuroblastoma derived (avian)	*Mycn*	NM_008709
A_55_P1972659	92.167643	2.336336372	Sperm acrosome associated 1	*Spaca1*	NM_026293
A_51_P428372	159.3257	2.296582165	Pro-platelet basic protein	*Ppbp*	NM_023785
A_51_P383270	42.49928125	2.178292966	Fraser syndrome 1 homolog (human)	*Fras1*	NM_175473
A_52_P1197913	6474.23205	2.169410999	Growth arrest and DNA-damage-inducible 45 beta	*Gadd45b*	NM_008655
A_52_P387884	127.717615	2.168260055	Predicted gene 7455	*Gm7455*	NM_001167923
A_55_P2106106	131.802971	2.165893492	G protein-coupled receptor 77	*Gpr77*	NM_001146005, NM_176912
A_55_P2109857	53454.46025	2.135840036	Regulator of G-protein signaling 2	*Rgs2*	NM_009061
A_51_P480190	130.0384485	2.109213448	Sperm acrosome associated 1	*Spaca1*	NM_026293
A_55_P2021187	361.9790825	2.107422241	Metastasis associated lung adenocarcinoma transcript 1 (non-coding RNA)	*Malat1*	NR_002847
A_52_P208649	552.684095	2.097820589	CART prepropeptide	*Cartpt*	NM_001081493, NM_013732
A_52_P300730	144.9705025	2.095584651	High mobility group AT-hook 2	*Hmga2*	NM_010441
A_55_P2165011	147.165	2.067882339	Fucosyltransferase 10	*Fut10*	NM_001012517, NM_134161
A_51_P408703	335.1278625	2.046457775	Ring finger protein 138 pseudogene	*1700045 I19Rik*	NR_003640
A_52_P156775	84.5671665	2.041447265	Secretoglobin, family 1C, member 1	*Scgb1c1*	NM_001099742
A_51_P520849	277.521115	2.028629638	Secreted frizzled-related protein 2	*Sfrp2*	NM_009144

for quantitative polymerase chain reaction [PCR]). Control mice were killed by inhalation of carbon dioxide, and the left adrenal glands were examined ($n=4$ for DNA microarray, $n=4$ for internal standard gene selection, $n=10$ for quantitative PCR). The isolated tissue was quickly soaked in 1.5 mL RNA later solution (Applied Biosystems, Carlsbad, CA).

DNA microarray

Total RNA was extracted from the tissue using an RNeasy Mini Kit (Qiagen, Valencia, CA). The quality of RNA was determined by electrophoresis on a 1% agarose gel and ethidium bromide staining. All the microarray analysis procedures described here were performed at Tohoku Chemical Research Institute of Bio-system Informatics (Morioka, Japan), by following the manufacturer's instructions. The quality of RNA was confirmed with 2100 bioanalyzer (Agilent Technologies, Santa Clara, CA) in which the 18S and 28S ribosomal bands were clearly visible. Gene expression profiles were determined using the Mouse GE 4x44K v2 Microarray Kit (four arrays; Agilent Technologies).

Quality control. Quality control of the feature was performed using the settings recommended by Agilent Technologies. The background was subtracted, and the signal intensity of each gene was globally normalized using locally weighted scatterplot smoothing. The following flag parameters were used, "Feature is saturated"; "Feature is not uniform"; "Feature is not positive and significant"; "Feature is not above background"; "Feature is a population outlier"; "Is control type." To these parameters, the following words were applied:

Detected: The data are reliable.
Not detected: The quality of data are undetermined.
Compromised: The data are unreliable.
Thereafter, to each spot (four spots per gene), the following words were applied:
Detected: All the parameters are "Detected."
Not detected: The parameters are combinations of "Detected" and "Not detected."
Compromised: One of the parameters is "Compromised."
For further analyses, we used genes whose spots in all four arrays were judged "Detected" or "Not detected."

Table 2. Downregulated Genes of the Adrenal Gland Arranged by Increasing Fold Change

Probe name	*Signal intensity in control*	*Fold change*	*Description*	*Symbol*	*RefSeq*
A_55_P2131060	168.3795875	0.178329922	RIKEN cDNA 9530053H05 gene	*9530053 H05Rik*	XR_035210, XR_035293
A_55_P2099594	824.53906	0.307055213	Stearoyl-coenzyme A desaturase 3	*Scd3*	NM_024450
A_52_P494622	2017.130193	0.330711587	Nuclear receptor subfamily 4, group A, member 2	*Nr4a2*	NM_001139509, NM_013613
A_55_P2032079	32104.70025	0.35226682	D site albumin promoter binding protein	*Dbp*	NM_016974
A_51_P258493	99.82523375	0.358234304	Period homolog 3 (Drosophila)	*Per3*	NM_011067
A_51_P453909	1126.981645	0.361199024	Cytochrome P450, family 2, subfamily f, polypeptide 2	*Cyp2f2*	NM_007817
A_51_P285097	61.15388375	0.382524007	WD repeat domain 38	*Wdr38*	NM_029687
A_55_P2279807	416.3360175	0.382598282	RIKEN cDNA 6720427I07 gene	*6720427 I07Rik*	
A_55_P2032081	25812.0535	0.39276457	D site albumin promoter binding protein	*Dbp*	NM_016974
A_55_P2057283	375.8735675	0.413693444			
A_55_P2336173	240.99968	0.419199325	miRNA containing gene	*Mirg*	NR_028265
A_55_P2276224	35.5700205	0.424322034	RIKEN cDNA 9330175E14 gene	*9330175 E14Rik*	NR_015514
A_55_P2042600	31.76226	0.424427694			
A_51_P483576	579.4216775	0.427562195			
A_55_P1998781	489.6958875	0.448673039	Zinc finger, CCHC domain containing 16	*Zcchc16*	NM_001033795
A_52_P70796	49.50055725	0.449355635	Chemokine (C-X-C motif) receptor 5	*Cxcr5*	NM_007551
A_51_P141546	1110.49385	0.451334792	Orosomucoid 2	*Orm2*	NM_011016
A_55_P1993723	31.07631925	0.456494379	Acyl-CoA synthetase bubblegum family member 2	*Acsbg2*	NM_001039114
A_66_P126254	57.31831925	0.463060628	Growth differentiation factor 7	*Gdf7*	NM_013527
A_55_P2145224	460.22919	0.46928739			
A_55_P2045007	297.637785	0.471485269	Histamine receptor H1	*Hrh1*	NM_008285
A_52_P223809	1032.715463	0.476333823	DEXH (Asp-Glu-X-His) box polypeptide 58	*Dhx58*	NM_030150
A_51_P272066	249.033675	0.476399003	RIKEN cDNA 2010109I03 gene	*2010109 I03Rik*	NM_025929
A_55_P2032553	29.48496325	0.483244729	RIKEN cDNA 9430024F10 gene	*9430024 F10Rik*	XM_001475368, XM_001477010
A_51_P501844	325.4883775	0.483703037	Cytochrome P450, family 26, subfamily b, polypeptide 1	*Cyp26b1*	NM_001177713, NM_175475
A_55_P1976097	1322.081375	0.490770113			
A_51_P489903	382.17449	0.493797658	8-Oxoguanine DNA-glycosylase 1	*Ogg1*	NM_010957
A_52_P483336	190.7524985	0.496741195	Membrane-spanning 4-domains, subfamily A, member 1	*Ms4a1*	NM_007641

Table 3. Upregulated Genes of the Adrenal Gland Arranged by Decreasing Signal Intensity in Hypothermia

Probe name	*Signal intensity in hypothermia*	*Fold change*	*Description*	*Symbol*	*RefSeq*
A_55_P2186672	156486.4275	1.488810051	Ribosomal protein S14	*Rps14*	NM_020600
A_55_P2100241	153603.9675	1.426390105	18S ribosomal RNA	*Rn18s*	NR_003278
A_55_P2155397	124816.2675	1.191423235	Ribosomal protein S8	*Rps8*	NM_009098
A_55_P2075479	119471.2265	1.120064513	Ribosomal protein L37a	*Rpl37a*	NM_009084
A_55_P2005081	115094.861	1.16827317	Ribosomal protein 10	*Rpl10*	NM_052835
A_65_P06061	113780.865	1.128924293	Ribosomal protein L37	*Rpl37*	NM_026069
A_55_P1957204	113700.391	1.16674735	60S ribosomal protein L37a pseudogene	*Gm4613*	XM_001480907, XM_003086576
A_55_P2031407	112166.954	1.118366638			
A_55_P1968606	110572.7025	1.143552761	Synergin, gamma	*Synrg*	NM_001115009, NM_194341
A_55_P2017774	109469.8235	1.05123966	Tumor protein, translationally-controlled 1 pseudogene	*Gm6790*	
A_55_P2149020	104690.6775	1.216695405	Ribosomal protein L35	*Rpl35*	NM_025592
A_55_P2051047	104395.0235	1.223220678	Ribosomal protein S10	*Rps10*	NM_025963
A_55_P2069955	102331.1875	1.254554522	Predicted gene 10063	*Gm10063*	XM_001472702, XM_001479052
A_55_P2029344	101309.1715	1.327089867	Ribosomal protein L23	*Rpl23*	NM_022891
A_55_P1956063	97570.2825	1.201758644	Phenazine biosynthesis-like protein domain containing 1	*Pbld1*	NM_026701
A_55_P2032600	97392.31625	1.146596023	Ribosomal protein S24	*Rps24*	NM_207634, NM_207635, NM_011297
A_55_P2121543	95240.2825	1.163873748	Ribosomal protein S20	*Rps20*	NM_026147
A_55_P2036380	94962.8675	1.106775996	Predicted gene 6440	*Gm6440*	XM_001475978, XM_001480472
A_55_P2036317	94943.79	1.088073172	Predicted gene 12508	*Gm12508*	XM_001476155, XM_003086360
A_55_P1985519	94799.48875	1.193554736			
A_55_P1972841	93821.40375	1.10473156	Ribosomal protein S28	*Rps28*	NM_016844
A_55_P1963080	93032.637	1.156605654	Ribosomal protein S12	*Rps12*	NM_011295
A_55_P2147816	92060.589	1.111752971	Predicted gene 4945	*Gm4945*	XM_140042, XM_911987
A_55_P1955059	90800.6125	1.136032289	Ribosomal protein L38	*Rpl38*	NM_001048058, NM_023372, NM_001048057
A_55_P2090953	90086.0225	1.124439929			
A_55_P2137773	89968.943	1.158127307	Ribosomal protein S24, pseudogene 3	*Rps24-ps3*	
A_55_P1969197	89632.935	1.06923572			
A_55_P2091308	89180.44	1.137855913	Ribosomal protein L38	*Rpl38*	NM_001048058, NM_023372, NM_001048057
A_55_P2027640	89123.50375	1.062687562			
A_55_P2070913	88047.0175	1.11888157	Ribosomal protein L14	*Rpl14*	NM_025974
A_55_P1971513	87544.2835	1.198585213	Predicted gene 3649	*Gm3649*	XM_001477499
A_55_P2186787	87360.4375	1.142197047	Ribosomal protein L29, pseudogene 5	*Rpl29-ps5*	
A_51_P488673	85356.04	1.162644159	Guanine nucleotide binding protein (G protein), beta polypeptide 2 like 1	*Gnb2l1*	NM_008143
A_55_P2081885	84246.58525	1.183050952			
A_55_P2152246	83867.6	1.105824247	60S ribosomal protein L19-like	*LOC100045367*	XM_001472605
A_55_P2081168	83536.6075	1.233369179	Ribosomal protein L7	*Rpl7*	NM_011291
A_55_P2020962	83157.31325	1.086690232			
A_55_P2131577	81956.07625	1.103668786			
A_55_P2149049	81568.18625	1.212224184	Ribosomal protein L32	*Rpl32*	NM_172086
A_55_P1977422	81566.75425	1.15275634			

Table 4. Downregulated Genes of the Adrenal Gland Arranged by Decreasing Signal Intensity in Control Mice

Probe name	*Signal intensity in control*	*Fold change*	*Description*	*Symbol*	*RefSeq*
A_55_P1976754	135680.6275	0.903646452	Peptidylprolyl isomerase A	*Ppia*	NM_008907, XR_105433, XR_106634
A_55_P2145879	130507.28	0.966409459	Tumor protein, translationally-controlled 1	*Tpt1*	NM_009429
A_55_P2164221	116394.2215	0.936017092	Tumor protein, translationally-controlled 1	*Tpt1*	NM_009429
A_55_P2083649	112980.2575	0.644204481	Aminolevulinic acid synthase 1	*Alas1*	NM_020559
A_55_P2020577	103924.789	0.897106009	Procollagen C-endopeptidase enhancer protein	*Pcolce*	NM_008788
A_55_P1970596	93686.65625	0.926328958			
A_51_P406020	90533.96375	0.8467639	Abhydrolase domain containing 4	*Abhd4*	NM_001205181, NM_134076
A_51_P401958	86200.02975	0.708742786	Transaldolase 1	*Taldo1*	NM_011528
A_55_P2128224	81730.9485	0.899824361			
A_55_P2154132	78857.0075	0.900185505	Tubulin, alpha 1B	*Tuba1b*	NM_011654
A_55_P2005343	75403.6565	0.878915735			
A_52_P165654	74943.8125	0.759726779	Steroidogenic acute regulatory protein	*Star*	NM_011485
A_55_P1970866	73840.505	0.887125076	Ribosomal protein, large, P0	*Rplp0*	NM_007475
A_55_P1964682	73161.505	0.842091397	28S ribosomal RNA	*LOC236598*	NR_003279
A_55_P2125743	71455.7715	0.845233141	Predicted gene 8842	*Gm8842*	XM_001003664, XM_001004356
A_55_P2009588	70942.98575	0.94324249	Ribosomal protein L13	*Rpl13*	NM_016738
A_55_P2053456	66709.12625	0.960983337	Eukaryotic translation elongation factor 1 alpha 1 pseudogene	*Gm6548*	NR_003363
A_55_P2074776	62393.11925	0.905969075	Predicted gene 8894	*Gm8894*	XM_993473
A_55_P2154173	61721.538	0.886727012	Predicted pseudogene 5526	*Gm5526*	XM_484859, XM_905351
A_55_P2095000	61561.15425	0.949181745			
A_55_P1988328	61501.83525	0.925325395			
A_55_P2093483	60268.91525	0.907875661			
A_55_P2146749	59694.05475	0.947401171	Ribosomal protein S13	*Rps13*	NM_026533
A_55_P2027969	59355.21275	0.918401863	Myosin, light polypeptide 6, alkali, smooth muscle and non-muscle	*Myl6*	NM_010860
A_55_P1986541	59095.67525	0.963033232	Ribosomal protein S11 pseudogene	*Gm9808*	XM_001473056, XM_003085817
A_55_P2011237	58786.23025	0.912951509			
A_55_P2139665	57145.60575	0.883549734	40S ribosomal protein S2-like	*LOC639606*	XM_003084649, XM_917948
A_55_P2171047	56251	0.916720258	Ornithine decarboxylase antizyme 1	*Oaz1*	NM_008753
A_55_P2081133	55989.5425	0.837152024	Glyceraldehyde-3-phosphate dehydrogenase	*Gapdh*	NM_008084
A_55_P2114994	55602.03975	0.895901246			
A_55_P1990859	55241.465	0.917703232	Ribosomal protein L6	*Rpl6*	NM_011290
A_55_P1995210	55040.7595	0.94155868	Predicted gene 11849	*Gm11849*	XM_001474209, XM_001475013
A_55_P2140955	54853.09275	0.868671223			
A_51_P237752	53759.53325	0.88600706	Polymerase I and transcript release factor	*Ptrf*	NM_008986
A_55_P2038077	53105.72875	0.866228347	Ribosomal protein SA	*Rpsa*	NM_011029
A_55_P2081482	52454.42925	0.880517981	ATP synthase, H+ transporting, mitochondrial F0 complex, subunit C2 (subunit 9)	*Atp5g2*	NM_026468
A_55_P2011235	52026.015	0.860201797	Ribosomal protein L13	*Rpl13*	NM_016738
A_55_P2033927	51976.148	0.928282329	Predicted gene 5528	*Gm5528*	XM_484880, XM_910525
A_55_P1993629	50949.8695	0.815733383			
A_55_P2042481	50073.191	0.90505848	Ribsomal protein S2 pseudogene	*Gm10653*	NR_003965

Selection of significantly regulated genes. For selecting significantly regulated genes, the one sample Student's *t*-test was performed. p Values of 0.05 or less were considered statistically significant. The correction for multiple tests (Benjamini-Hochberg method) was not performed, because we thought that the selected genes would be extremely few in number.

Gene set analysis. Using the GenMAPP pathway database and previously published methods (Kim and Volsky, 2005), gene set analysis was performed. The mean of fold changes among all significantly regulated genes, and the fold change of each gene set, were compared. Z scores of fold changes were calculated, and statistical analyses with standard normal distribution were performed.

p Values of 0.05 or less were considered statistically significant.

Gene functional category analysis. Gene functional category analyses were performed. The number of genes corresponding to each Gene Ontology term among all genes was compared to the number among significantly regulated genes using Fisher's Exact Test. p Values of 0.05 or less were considered statistically significant.

Quantitative PCR

To validate selected aspects of microarray results, three upregulated genes, shown on Table 1 (FBJ osteosarcoma oncogene: *Fos*, C2 calcium-dependent domain containing 4B: *C2cd4b*, regulator of G-protein signaling 1: *Rgs 1*) and three downregulated genes, shown on Table 2 (stearoyl coenzyme A desaturase 3: *Scd 3*, nuclear receptor subfamily 4, group A, member 2: *Nr4a2*, D site albumin promoter binding protein: *Dbp*) were selected for measurement by quantitative PCR.

RNA extraction and reverse transcription. Total RNA was extracted from tissues using an RNeasy Mini Kit (Qiagen). The quality of RNA was evaluated using electrophoresis on a 1% agarose gel and staining with ethidium bromide. The RNA was treated with TURBO DNase (Applied Biosystems). cDNA was synthesized using a High Capacity cDNA reverse

Table 5. Gene Set Analysis of the Adrenal Gland

GenMAPP	*Number of genes*	p-*Value*	*Fold change average*	Z *score*
Mm_Smooth_muscle_contraction	41	5.76E-08	0.327	5.426
Mm_TGF_Beta_Signaling_Pathway	13	3.49E-06	0.491	4.640
Mm_MAPK_signaling_pathway_KEGG	40	2.86E-05	0.258	4.184
Mm_TGF-beta-Receptor_NetPath_7	51	3.77E-05	0.227	4.121
Mm_Selenium-metabolism_Selenoproteins	12	1.26E-04	0.424	3.834
Mm_GPCRDB_Class_A_Rhodopsin-like	13	7.23E-04	0.361	3.381
Mm_Calcium_regulation_in_cardiac_cells	31	1.76E-03	0.221	3.128
Mm_TNF-alpha-NF-kB_NetPath_9	56	1.36E-02	−0.112	−2.466
Mm_Ribosomal_Proteins	63	2.69E-02	0.115	2.213
Mm_ESC_Pluripotency_Pathways	30	0.058539123	0.140	1.892
Mm_B_Cell_Receptor_NetPath_12	40	0.060173826	−0.100	−1.880
Mm_T-Cell-Receptor_NetPath_11	28	0.063005168	0.142	1.859
Mm_IL-6_NetPath_18	22	0.073984526	0.153	1.787
Mm_Regulation_of_Actin_Cytoskeleton_KEGG	32	0.075333233	−0.106	−1.778
Mm_Alpha6-Beta4-Integrin_NetPath_1	24	0.081785532	0.144	1.740
Mm_EGFR1_NetPath_4	42	0.085953468	0.110	1.717
Mm_Insulin_Signaling	47	0.096395054	0.102	1.663
Mm_Apoptosis	20	0.121537908	−0.118	−1.548
Mm_IL-7_NetPath_19	12	0.135364454	−0.150	−1.493
Mm_p38_MAPK_signaling_pathway	11	0.187818954	−0.137	−1.317
Mm_Integrin-mediated_cell_adhesion_KEGG	27	0.202880461	−0.080	−1.273
Mm_IL-3_NetPath_15	23	0.230323616	−0.082	−1.200
Mm_Proteasome_Degradation	31	0.236472278	−0.068	−1.184
Mm_G13_Signaling_Pathway	15	0.248969427	−0.100	−1.153
Mm_Adipogenesis	19	0.262757145	0.107	1.120
Mm_Delta-Notch_NetPath_3	20	0.277918303	−0.079	−1.085
Mm_Androgen-Receptor_NetPath_2	38	0.374440936	−0.042	−0.888
Mm_Id_NetPath_5	14	0.38062277	0.099	0.877
Mm_IL-2_NetPath_14	15	0.424082909	−0.066	−0.799
Mm_Wnt_NetPath_8	40	0.427676548	0.058	0.793
Mm_RNA_transcription_Reactome	15	0.448815321	−0.062	−0.757
Mm_Circadian_Exercise	20	0.493625081	0.068	0.685
Mm_mRNA_processing_binding_Reactome	145	0.514750248	−0.009	−0.651
Mm_G_Protein_Signaling	24	0.517853774	0.060	0.647
Mm_Focal_adhesion_KEGG	41	0.565007006	−0.022	−0.575
Mm_Wnt_Signaling	18	0.56524677	0.062	0.575
Mm_Cell_Cycle_KEGG	17	0.574692992	0.062	0.561
Mm_Translation_Factors	27	0.576961178	−0.029	−0.558
Mm_IL-5_NetPath_17	16	0.884339019	0.025	0.145
Mm_IL-4_NetPath_16	14	0.915237134	0.001	−0.106
Mm_Fas_Pathway_and_Stress_Induction of_HSP_Regulation_Biocarta	11	0.927751985	0.001	−0.091
Mm_Cell_Cycle-G1_to_S_control_Reactome	15	0.943787969	0.018	0.071
Mm_IL-1_NetPath_13	12	0.962413047	0.006	−0.047
Mm_Kit-Receptor_NetPath_6	11	0.964151772	0.016	0.045

transcription kit with RNase inhibitor (Applied Biosystems), by following the manufacturer's instructions.

Real-time quantitative PCR. TaqMan Gene Expression Assays (Applied Biosystems) were used for the following primers and probe (*Fos*: Mm00487425_m1, *C2cd4b*: Mm01179276_g1, *Rgs1*: Mm00450170_m1, *Scd3*: Mm00470480_m1, *Nr4a2*: Mm00443060_m1, *Dbp*: Mm00497539_m1). For selecting the internal standard gene, the internal standard gene stability value was used (Vandesompele *et al.*, 2002); those of β-actin, glyceraldehyde-3-phosphate dehydrogenase, and 18S ribosomal RNA were 1.55, 1.89, and 1.95, respectively. Therefore, β-actin was employed as the internal standard. The β-actin primers and probe were supplied with TaqMan Gene Expression Assays (Mm00607939_s1, Applied Biosystems). Real-time quantitative PCR was performed using PRISM 7500 sequence detector (Applied Biosystems). A 50 μL reaction mixture containing TaqMan Gene Expression Master Mix (Applied Biosystems) was used, and thermal cycler conditions given in the manufacturer's instructions were followed. All samples were analyzed in triplicate. The relative expression of the target gene was calculated by the $\Delta\Delta$ Ct method, as described by the manufacturer (Applied Biosystems). Differences in gene expression between control and hypothermic adrenal glands were analyzed using the Student's t test, and p values of 0.05 or less were considered statistically significant.

The research described in this report was conducted in accordance with the guidelines for animal experimentation, Iwate Medical University.

Results

DNA microarray

Quality control. From 39,429 genes on the microarray plate, we selected 23,905 genes for further analysis.

Selection of the significantly regulated genes. We identified a total of 4051 significantly expressed genes; 2015 were upregulated, and 2036 were downregulated, in hypothermic mouse adrenal gland tissue. Of the upregulated genes, 36 genes increased >2-fold, 6 >4-fold, 3 >6-fold, 1 >8-fold, and 2 >10-fold. *Fos* was the most upregulated gene, with a 33.7-fold increase. Of downregulated genes, compared to levels in control mice, 19 were <0.5-fold, 8<0.4-fold, and 1<0.2-fold. *Scd3* was the most downregulated gene, with a 0.307-fold reduction. Upregulated genes and downregulated genes were arranged in descending and ascending orders of fold change, respectively. Table 1 lists 48 genes having a more than two-fold change, and the 28 genes that had a less than 0.5-fold change are shown in Table 2.

In addition, upregulated and downregulated genes were also arranged in descending order of signal intensity. Table 3

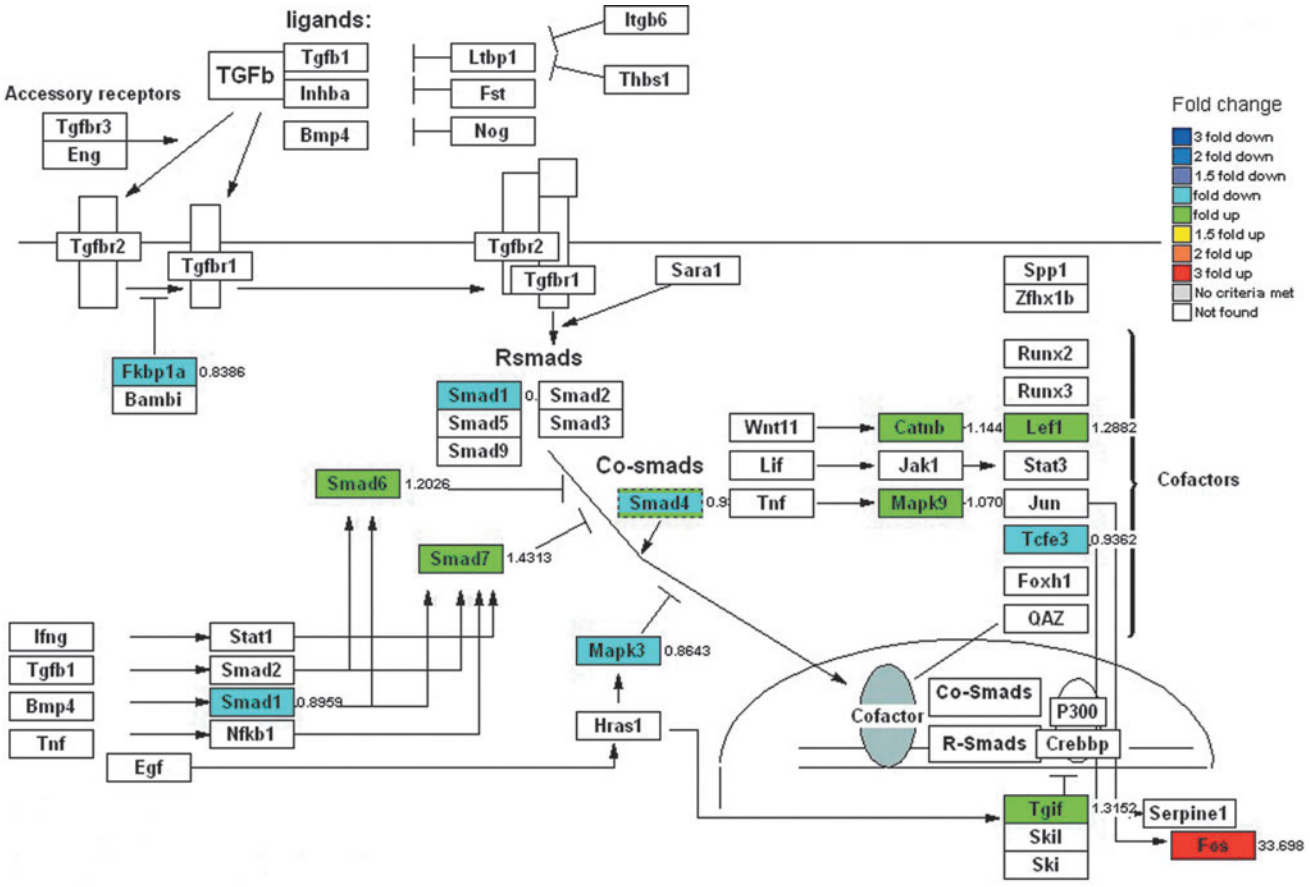

FIG. 1. Transforming growth factor β (TGF-β) signaling pathway in hypothermia. *Fos*, which is the most upregulated gene, is found in this pathway.

shows 40 upregulated genes that had a signal intensity of more than 80,000 in hypothermia, whereas 40 downregulated genes that had a signal intensity of more than 50,000 in controls are listed in Table 4.

Gene set analysis. The significantly enriched gene sets that were upregulated or downregulated are summarized in Table 5. A total of nine significant pathways ($p < 0.05$) were identified, and transforming growth factor-β (TGF-β), and tumor necrosis factor-α (TNF-α) could be involved in the pathogenesis of hypothermia. In addition, the pathway through which TGF-β would induce *Fos,* the most upregulated gene in the present study, was identified by this analysis (Fig. 1).

Gene functional category analysis. To investigate the biological functions involving the discriminating genes, we performed Gene Ontology category analysis. For increased (Table 6) and decreased genes (Table 7), the top 10 categories of biological process, molecular function, and cellular component were demonstrated. The most overexpressed categories in upregulated and downregulated genes were cellular process, binding, and cell and cell part.

Validation of gene expression results by quantitative PCR

Validation by quantitative PCR of three upregulated (Fig. 2) and three downregulated (Fig. 3) genes was performed. Results obtained by DNA microarray and quantitative PCR were consistent, although levels of differences detected by the two methods were not exactly the same. Of the downregulated genes, *Dbp* was decreased to a greater extent than was *Nr4a2*.

Discussion

In association with hypothermia, molecular biological analyses have revealed inductions of mRNA in the hypothalamus (Umehara *et al.*, 2011), lung, heart, liver, and kidney (Cullen and Sarge, 1997). In addition, studies have been carried out concerning adrenal hormones in hypothermia. It was demonstrated that plasma noradrenaline and adrenaline values were significantly lower in the hypothermia group than in the control group (Hirvonen and Lapinlampi, 1989). This reaction might be due to cold stress, causing noradrenaline and adrenaline to appear in the blood and urine in the

Table 6. Gene Ontology Classification of Upregulated Genes

GO accession	*GO term*	*Count in total*	*Count in selection*	p *Value*
Biological process				
GO:0009987|GO:0008151| GO:0050875	Cellular process	9212	773	4.11E-17
GO:0008152	Metabolic process	7363	651	4.75E-18
GO:0044237	Cellular metabolic process	5717	530	1.69E-17
GO:0044238	Primary metabolic process	5722	529	3.06E-17
GO:0043170|GO:0043283	Macromolecule metabolic process	4448	457	9.59E-23
GO:0044260|GO:0034960	Cellular macromolecule metabolic process	3964	427	1.68E-24
GO:0019222	Regulation of metabolic process	3453	340	5.84E-13
GO:0006807	Nitrogen compound metabolic process	3292	317	1.24E-10
GO:0034641	Cellular nitrogen compound metabolic process	3208	310	1.58E-10
GO:0006139|GO:0055134	Nucleobase, nucleoside, nucleotide and nucleic acid metabolic process	2974	300	2.17E-12
Molecular function				
GO:0005488	Binding	10078	833	1.71E-17
GO:0005515|GO:0045308	Protein binding	5306	437	7.94E-06
GO:0003824	Catalytic activity	4782	382	0.00189936
GO:0043167	Ion binding	3145	288	3.53E-07
GO:0043169	Cation binding	3136	287	3.99E-07
GO:0046872	Metal ion binding	3101	284	4.60E-07
GO:0003676	Nucleic acid binding	2349	240	4.82E-10
GO:0003677	DNA binding	1611	160	2.85E-05
GO:0046914	Transition metal ion binding	1531	141	0.00734583
GO:0008270	Zinc ion binding	1308	127	0.00189936
Cellular component				
GO:0005623	Cell	13909	1040	3.19E-10
GO:0044464	Cell part	13908	1040	3.19E-10
GO:0005622	Intracellular	9579	827	4.85E-23
GO:0044424	Intracellular part	9346	811	4.85E-23
GO:0043226	Organelle	7946	709	7.12E-22
GO:0043229	Intracellular organelle	7921	708	5.62E-22
GO:0043227	Membrane-bounded organelle	7007	634	8.56E-20
GO:0043231	Intracellular membrane-bounded organelle	6995	632	1.31E-19
GO:0005737	Cytoplasm	6628	558	3.35E-10
GO:0005634	Nucleus	4084	408	1.60E-17

Table 7. Gene Ontology Classification of Downregulated Genes

GO accession	*GO term*	*Count in total*	*Count in selection*	p *Value*
Biological process				
GO:0009987|GO:0008151| GO:0050875	Cellular process	9212	842	5.61E-35
GO:0008152	Metabolic process	7363	709	9.66E-34
GO:0044237	Cellular metabolic process	5717	590	3.13E-34
GO:0044238	Primary metabolic process	5722	584	2.52E-32
GO:0043170|GO:0043283	Macromolecule metabolic process	4448	471	9.08E-28
GO:0044260|GO:0034960	Cellular macromolecule metabolic process	3964	442	1.13E-30
GO:0006807	Nitrogen compound metabolic process	3292	350	3.74E-19
GO:0034641	Cellular nitrogen compound metabolic process	3208	347	3.18E-20
GO:0019222	Regulation of metabolic process	3453	342	6.50E-14
GO:0006139|GO:0055134	Nucleobase, nucleoside, nucleotide and nucleic acid metabolic process	2974	320	6.18E-18
Molecular function				
GO:0005488	Binding	10078	864	2.66E-25
GO:0005515|GO:0045308	Protein binding	5306	477	4.12E-13
GO:0003824	Catalytic activity	4782	418	4.25E-09
GO:0003676	Nucleic acid binding	2349	254	6.96E-14
GO:0000166	Nucleotide binding	2011	214	1.13E-10
GO:0016787	Hydrolase activity	2050	187	3.41E-04
GO:0017076	Purine nucleotide binding	1746	175	1.99E-06
GO:0032555	Purine ribonucleotide binding	1674	172	5.17E-07
GO:0032553	Ribonucleotide binding	1675	172	5.32E-07
GO:0003677	DNA binding	1611	163	3.60E-06
Cellular component				
GO:0044464	Cell part	13908	1119	1.08E-28
GO:0005623	Cell	13909	1119	1.08E-28
GO:0005622	Intracellular	9579	962	0
GO:0044424	Intracellular part	9346	949	0
GO:0043229	Intracellular organelle	7921	806	0
GO:0043226	Organelle	7946	806	0
GO:0043231	Intracellular membrane-bounded organelle	6995	736	0
GO:0043227	Membrane-bounded organelle	7007	736	0
GO:0005737	Cytoplasm	6628	693	0
GO:0005634	Nucleus	4084	468	5.21E-36

early stages, but then decline as the adrenals become exhausted (Hirvonen and Huttunen, 1995; Saukko and Knight, 2004). In addition, cortisol has been reported to remain low in hypothermia (Woolf *et al.*, 1972). Likewise, no variations of noradrenaline, adrenaline, or cortisol pathways were observed in the present study. Although adrenal responsiveness is thought to decrease in hypothermia (Felicetta *et al.*, 1980), DNA microarray analyses in the present study revealed acute adrenal responses. The potential biomarkers revealed would be *Fos*, *C2cd4b*, and *Rgs1* from among the upregulated genes (Table 1), and *Scd3*, *Nr4a2*, and *Dbp* from among the downregulated genes (Table 2). Needless to say, the possibility exists that other genes that expressed differentially may be useful for diagnosing hypothermia. We also arranged upregulated and downregulated genes in descending order of signal intensity (Tables 3 and 4). However, these genes showed few changes.

Biomarkers specific to hypothermia would be ideal for use in daily forensic practice. However, it is impossible to check the dynamics of biomarker candidates in all pathophysiologic conditions and deaths, and to validate their specificities. Aspects of the mechanism of death remain unknown. We consider that autopsies are the mainstay in death investigation, and that biomarkers would provide a supplementary source of information. In addition, most autopsy findings of hypothermia, including bright pink lividity, minute hemorrhage of gastric mucosa, and acetone detection, are not specific to hypothermia; this poses difficulties for researching the condition. Although tumor markers are not specific for only one tumor type, they play an active part in the field of oncology. We believe that biomarker utilization could be beneficial for development in the field of forensic pathologic investigation.

In connection with hypothermia, no reports of changes in *C2cd4b*, *Rgs 1*, *Scd3*, *Nr4a2*, or *Dbp* expression were found. On the other hand, *Fos* is a multifaceted gene, expressed during cell growth, differentiation, and development (Muller, 1986; Tulchinsky, 2000). In this study, *Fos* was acutely upregulated during hypothermia. Furthermore, there have been many studies showing that various types of noxious stimuli, (including thermal, mechanical, and chemical) induce expression of *Fos* in the brain and spinal cord (Morgan and Curran, 1991; Herrera and Robertson, 1996).

Results of the current the pathway analysis suggest that TNF-α and TGF-β are associated with the pathogenesis of hypothermia. The present study also suggests that TGF-β would promote the expression of *Fos*, which was the most

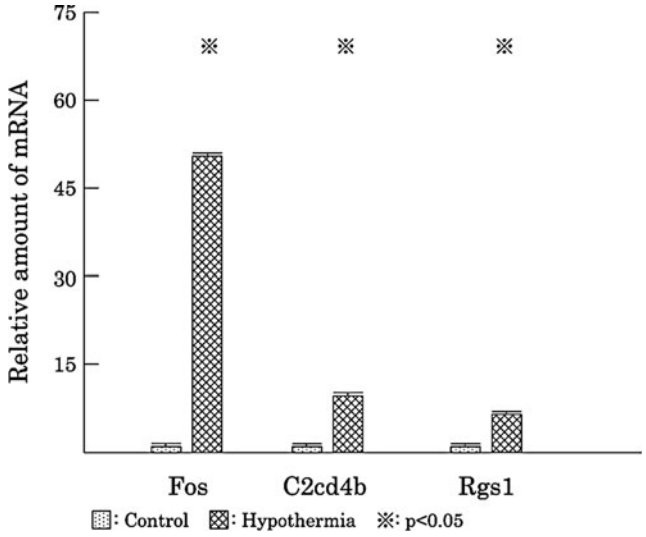

FIG. 2. Real-time quantitative polymerase chain reaction (PCR) analysis of upregulated genes. mRNA levels in hypothermia relative to control. Values are expressed as mean ± standard deviation (SD).

upregulated gene. However, although the production of TGF-β in the adrenal gland was reported (Ho and Vinson, 1995; Langlois *et al.*, 1998; Otsuka *et al.*, 1999), relationships between TGF-β and *Fos* could not be assessed in the present study. Therefore, this is simply a hypothesis. In addition, the detailed mechanisms of TNF-α activity in the adrenal gland remain unexplained. In the Gene Ontology analysis, cellular process, binding, cell, and cell part were overexpressed categories. These results can not directly contribute to detection of hypothermia biomarkers. However, we can compare the present Gene Ontology terms with those of other organs involved in hypothermia, and consider both along with other research developments. Analyzing common Gene Ontology terms and

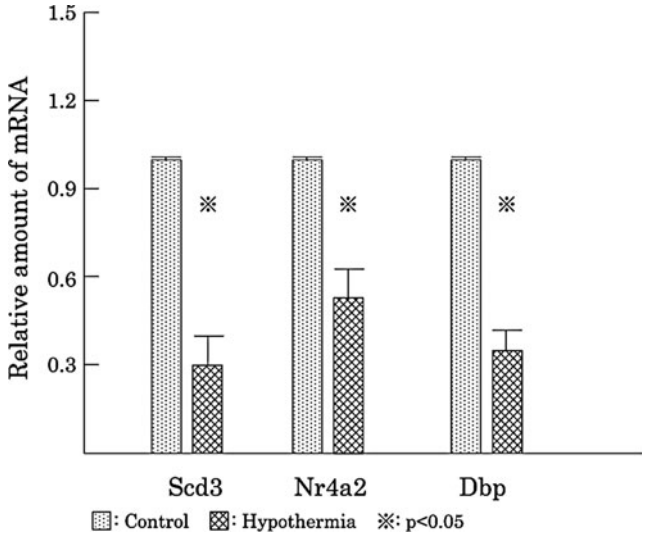

FIG. 3. Real-time quantitative PCR analysis of downregulated genes. mRNA levels in hypothermia relative to control. Values are expressed as mean ± SD.

organ-specific terms could help reveal the pathophysiology of hypothermia in the future.

The present research demonstrated changes in gene expression in the hypothermic mouse adrenal gland, and we suggest that mRNA expressions may be useful for the diagnosis of hypothermia. However, reports of forensic hypothermia investigations using molecular biological methods have only recently begun to appear, and existing hypothermia findings are also important (Turk, 2010). In addition, fatty degeneration of renal tubular epithelium (Preuss *et al.*, 2004) and myocardial cells (Preuss *et al.*, 2006), vacuoles in pancreatic adenoid cells (Preuss *et al.*, 2007), and heat shock protein 70 in renal tubular epithelium and glomerular podocytes (Preuss *et al.*, 2008) can be used as markers of hypothermia. In forensic practice, considering the combination of macroscopic, microscopic, and molecular biologic observations would be conducive to a more accurate diagnosis of hypothermia.

DNA microarray analysis is used in many fields of medicine. In the present study of 23,905 genes, expression of only 48 genes increased more than two-fold, and that of only 28 genes decreased to less than 0.5-fold, of control levels. These results indicate that the practical uses of transcriptomic methods will be unavoidable in future forensic pathologic research. Since the standardization of experimental conditions is an absolute requirement for transcriptomic analsyses, its application for analysis of human forensic samples would be meaningless. For detailed analysis of pathophysiology and forensic biomarker identification, animal experimentation in conjunction with transcriptomic analysis would play important roles. After considering animal transcriptomic data along with postmortem changes, expression of biomarker candidates in forensic human samples should be assessed. Since RNA would decompose in the postmortem interval, utilization of protein levels should be considered for daily forensic practice. In other words, protein analysis would be the next stage after DNA microarray analysis. However, murine adrenal glands are extremely small, and we think that the reliability of antibodies currently on the market is not guaranteed (Pradidarcheep *et al.*, 2008, 2009; Bordeaux *et al.*, 2010), or that no suitable antibodies could be found. Therefore, protein analysis involving immunohistochemistry was not performed in the present study. However, results of the present murine DNA microarray study may provide data applicable to development of future immunohistochemical analysis of human samples. Data presented in this article could become the basis for further investigation. This article includes information regarding adrenal physiology during hypothermia, involving more than 20,000 genes. We believe that these data are informative, not only for future forensic pathological studies, but also potentially for clinical research into hypothermia. From the viewpoint of adrenal gene activity, they may contribute to elucidation of the pathophysiology of hypothermia.

Acknowledgment

This study was supported by JSPS KAKENHI Grant Number 24790641.

Disclosure Statement

All authors declare that they have no conflicts of interest.

References

Aghayev E, Thali MJ, Jackowski C, Sonnenschein M, Dirnhofer R, Yen K. MRI detects hemorrhages in the muscles of the back in hypothermia. Forensic Sci Int 2008;176:183–186.

Bordeaux J, Welsh A, Agarwal S, Killiam E, Baquero M, Hanna J, Anagnostou V, Rimm D. Antibody validation. Biotechniques 2010;48:197–209.

Cullen KE, Sarge KD. Characterization of hypothermia-induced cellular stress response in mouse tissues. J Biol Chem 1997; 272:1742–1746.

DiMaio VJ, DiMaio D. Hypothermia. In: Forensic pathology, 2nd ed. DiMaio VJ, DiMaio D (eds). Boca Raton, FL: CRC press, 2001, pp. 428–434.

Felicetta JV, Green WL, Goodner CJ. Decreased adrenal responsiveness in hypothermic patients. J Clin Endocrinol Metab 1980;50:93–97.

Herrera DG, Robertson HA. Activation of c-fos in the brain. Prog Neurobiol 1996;50:83–107.

Hirvonen J, Huttunen P. Increased urinary concentration of catecholamines in hypothermia deaths. J Forensic Sci 1982;27: 264–271.

Hirvonen J, Huttunen P. Hypothermia markers. Serum, urine, and adrenal gland catecholamines in hypothermic rats given ethanol. Forensic Sci Int 1995;72:125–133.

Hirvonen J, Lapinlampi T. Plasma and urine catecholamines and cerebral spinal fluid amine metabolites as hypothermia markers in Guinea-pigs. Med Sci Law 1989;29:130–135.

Ho MM, Vinson GP. Endocrine control of the distribution of basic fibroblast growth factor, insulin-like growth factor-I and transforming growth factor-beta 1 mRNAs in adult rat adrenals using non-radioactive *in situ* hybridization. J Endocrinol 1995;144:379–387.

Kim SY, Volsky DJ. PAGE: parametric analysis of gene set enrichment. BMC Bioinformatics 2005;6:144.

Langlois D, Le Roy C, Penhoat A, Lebrethon MC, Saez JM. Autocrine role of TGF beta 1 in adrenal. Horm Metab Res 1998;30:411–415.

Morgan JI, Curran T. Stimulus-transcription coupling in the nervous system: involvement of the inducible proto-oncogenes fos and jun. Annu Rev Neurosci 1991;14:421–451.

Muller R. Cellular and viral fos genes: structure, regulation of expression and biological properties of their encoded products. Biochim Biophys Acta 1986;823:207–225.

Okuda C, Saito A, Miyazaki M, Kuriyama K. Alteration of the turnover of dopamine and 5-hydroxytryptamine in rat brain associated with hypothermia. Pharmacol Biochem Behav 1986;24:79–83.

Otsuka F, Ogura T, Yamauchi T, Kataoka H, Kishida M, Miyatake N, Mimura Y, Kageyama J, Makino H. Long-term administration of adrenocorticotropin modulates the expression of IGF-I and TGF-beta 1 mRNAs in the rat adrenal cortex. Growth Horm IGF Res 1999;9:41–51.

Paton BC. Accidental hypothermia. Pharmacol Ther 1983;22: 331–377.

Pradidarcheep W, Labruyere WT, Dabhoiwala NF, Lamers WH. Lack of specificity of commercially available antisera: better specifications needed. J Histochem Cytochem 2008;56:1099–1111.

Pradidarcheep W, Stallen J, Labruyere WT, Dabhoiwala NF, Michel MC, Lamers WH. Lack of specificity of commercially available antisera against muscarinergic and adrenergic receptors. Naunyn Schmiedebergs Arch Pharmacol 2009;379: 397–402.

Preuss J, Dettmeyer R, Lignitz E, Madea B. Fatty degeneration in renal tubule epithelium in accidental hypothermia victims. Forensic Sci Int 2004;141:131–135.

Preuss J, Dettmeyer R, Lignitz E, Madea B. Fatty degeneration of myocardial cells as a sign of death due to hypothermia versus degenerative deposition of lipofuscin. Forensic Sci Int 2006; 159:1–5.

Preuss J, Dettmeyer R, Poster S, Lignitz E, Madea B. The expression of heat shock protein 70 in kidneys in cases of death due to hypothermia. Forensic Sci Int 2008;176:248–252.

Preuss J, Lignitz E, Dettmeyer R, Madea B. Pancreatic changes in cases of death due to hypothermia. Forensic Sci Int 2007; 166:194–198.

Saukko P, Knight B. Injury caused by cold: hypothermia. In: Knight's Forensic Pathology, 3rd ed. Saukko P, Knight B (eds). London: Arnold, 2004, pp. 414–420.

Tulchinsky E. Fos family members: regulation, structure and role in oncogenic transformation. Histol Histopathol 2000; 15:921–928.

Turk EE. Hypothermia. Forensic Sci Med Pathol 2010;6:106–115.

Ulrich AS, Rathlev NK. Hypothermia and localized cold injuries. Emerg Med Clin North Am 2004;22:281–298.

Umehara T, Usumoto Y, Tsuji A, Kudo K, Ikeda N. Expression of material mRNA in the hypothalamus and frontal cortex in a rat model of fatal hypothermia. Leg Med 2011;13:165–170.

Vandesompele J, De Preter K, Pattyn F, Poppe B, Van Roy N, De Paepe A, Speleman F. Accurate normalization of real-time quantitative RT-PCR data by geometric averaging of multiple internal control genes. Genome Biol 2002;3: RESEARCH0034.

Woolf PD, Hollander CS, Mitsuma T, Lee LA, Schalch DS. Accidental hypothermia: endocrine function during recovery. J Clin Endocrinol Metab 1972;34:460–466.

Address correspondence to:
Masataka Takamiya, MD, PhD
Department of Forensic Medicine
Iwate Medical University
2-1-1 Nishitokuta, Yahaba
Iwate 028-3694
Japan

E-mail: mtakamiy@iwate-med.ac.jp